

NATIONAL ADVISORY COMMITTEE FOR AERONAUTICS

15 DEC 1947

WARTIME REPORT

ORIGINALLY ISSUED
August 1941 as
Memorandum Report

STATIC CHARACTERISTICS OF HAMILTON STANDARD
PROPELLERS HAVING CLARK Y AND NACA 16-SERIES
BLADE SECTIONS

By Blake W. Corson, Jr., and Nicholas Mastrocola

Langley Memorial Aeronautical Laboratory
Langley Field, Va.

NACA

WASHINGTON NACA LIBRARY
LANGLEY MEMORIAL AERONAUTICAL
LABORATORY
Langley Field, Va.

NACA WARTIME REPORTS are reprints of papers originally issued to provide rapid distribution of advance research results to an authorized group requiring them for the war effort. They were previously held under a security status but are now unclassified. Some of these reports were not technically edited. All have been reproduced without change in order to expedite general distribution.

NATIONAL ADVISORY COMMITTEE FOR AERONAUTICS

MEMORANDUM REPORT

for the

Bureau of Aeronautics, Navy Department

STATIC CHARACTERISTICS OF HAMILTON STANDARD

PROPELLERS HAVING CLARK Y AND NACA 16-SERIES

BLADE SECTIONS

By Blake W. Corson, Jr., and Nicholas Mastrocola

SUMMARY

Static tests were made on two full-scale three-bladed propellers differing only in blade sections, at blade angles from 0° to 20° at the three-quarters radius. The tests were made out-doors under conditions of low wind velocity.

The data are analyzed on the basis of a static thrust figure of merit, and by Driggs' Simplified Propeller Calculations, which is a single-point method of reducing propeller data to airfoil data. Static propeller data are reduced first to airfoil data, then reconverted to propeller efficiency as a function of advance ratio for the purpose of comparing the NACA 16-series blade section with the Clark Y blade section.

A comparison of the efficiencies computed from static data indicates that a propeller having 16-series sections may give about three percent higher efficiency than a Clark Y propeller of similar blade form, when the blade sections operate at tip-speed ratios of about $M = 0.9$ or $M = 1.0$, at relatively high forward velocity. The propeller with Clark Y blade sections appears to be superior to that with the 16-series sections for take-off and climb.

INTRODUCTION

The tests described in this report constitute one phase of an investigation described in reference 1 to check flight tests made for the purpose of determining the relative merits of the

Clark Y and the 16-series sections. The tests were made on propellers operating under the condition of zero forward velocity. Thrust and power were measured at various propeller tip speeds and blade angle settings. The propellers used were two Hamilton-Standard three-bladed propellers identical in all respects except blade sections. One propeller embodied the Clark Y blade sections, the other was made with the NACA 16-series sections.

As the static test conditions can not be universally representative of conditions of application, the absolute values obtained from these tests are not highly significant. The results, however, can be very useful for making qualitative comparisons of propellers tested under identical conditions.

The purpose of this investigation was to determine the relative merits of the Clark Y propeller sections and the NACA 16-series sections at various propeller tip speeds. The propellers are compared on the basis of a static thrust-power figure of merit. As a further analysis, use is made of Driggs' Simplified Propeller Calculations, reference 2, for reducing the propeller characteristics to quasi airfoil characteristics. The airfoil polars so obtained are then reconverted into the propeller envelope efficiency as a function of the advance ratio.

This investigation was made at the request of the Bureau of Aeronautics, Navy Department. The testing was done on the static test equipment of the propeller-research section of the National Advisory Committee for Aeronautics at Langley Field, Virginia.

DESCRIPTION OF APPARATUS

Test rig.—The static propeller test rig used in this investigation, located out-doors, was essentially the same as that described in reference 3. The major difference in the set-up is that for the present tests an air-cooled radial engine furnished the motive power. This engine required a nacelle larger than that used in the earlier tests and of somewhat different shape. A photograph of the set-up is shown in figure 1, and a schematic diagram in figure 2.

Engine and nacelle.—In this series of tests the propeller was driven by a Pratt and Whitney R-1340 radial air-cooled engine. The power rating of this engine is 550 horsepower

at 2100 rpm. The propeller was driven directly at engine crank shaft speed and at low blade angles was turned up to 2300 rpm. The rotational speed of the engine and propeller was measured with a condenser tachometer which was not in error by more than $\pm 1/2$ percent, above 1000 rpm.

The engine cowling-nacelle combination was arranged to give as good cooling as was compatible with relatively low impedance to the propeller slipstream.

Propellers.— Two three-bladed Hamilton-Standard propellers differing only in blade section were investigated. The propeller designated by drawing number 6259A-18 was made with blade sections having the NACA 16-series airfoil profiles. These sections, described in reference 4, have relatively sharp leading and trailing edges, and have maximum thickness at the mid-chord station. They are designed to work efficiently at high speed by delaying the compressibility stall. The propeller identified by drawing number 6267A-18 had conventional Clark Y propeller sections. The blade form curves for both propellers are shown in figure 3. Blade sections at the 0.70 R are shown in figure 4. The section at the 0.70 R station rather than that at the 0.75 R was chosen because of the significance of the 0.70 R station in Driggs' method of propeller analysis.

TESTS

Each test was made at one blade angle setting. Beginning at about 600 rpm, the net thrust, torque, and propeller rotational speed were measured simultaneously at various intervals until the highest speed obtainable under 2300 rpm was reached. Readings were taken at speed intervals of about 100 rpm at low speeds, and at much smaller intervals near the top speed. Each propeller was tested at a series of blade angles from 0° to 20° by intervals of approximately two degrees. The blade angle was measured at the three-quarters radius. Before and after each run the wind velocity was measured with an anemometer. Tests were made only when the wind velocity was less than five miles per hour.

RESULTS

Coefficients and Symbols

The results of the static propeller tests are presented in terms of conventional coefficients.

$$C_T = \frac{T_e}{\rho n^2 D^4}, \text{ thrust coefficient}$$

$$C_P = \frac{P}{\rho n^3 D^5}, \text{ power coefficient}$$

$$T_e = T - \Delta D, \text{ effective thrust, pounds}$$

$$T, \text{ tension in propeller shaft, pounds}$$

$$\Delta D, \text{ the force exerted by the propeller slipstream on the nacelle and struts, pounds}$$

$$P = 2 \pi n Q, \text{ engine power, foot pounds per second}$$

$$Q, \text{ engine torque, pound-feet}$$

$$\rho, \text{ mass density of air, slugs per cubic foot}$$

$$n, \text{ propeller rotational speed, revolutions per second}$$

$$D = 2 R, \text{ propeller diameter, feet}$$

$$R, \text{ propeller tip radius, feet}$$

$$C_T/C_P, \text{ static thrust figure of merit}$$

$$M = \frac{\pi n D}{c}, \text{ tip-speed ratio}$$

$$c, \text{ speed of sound in air, feet per second}$$

$$J = V/nD, \text{ advance ratio}$$

$$V, \text{ air speed, feet per second}$$

$$\eta = \frac{C_T}{C_P} J, \text{ propeller efficiency}$$

$q = 1/2 \rho V^2$, dynamic pressure, pounds per square foot

L, lift, pounds

D, profile drag, pounds

S, area, square feet

$C_L = \frac{L}{q S}$, lift coefficient

$C_D = \frac{D}{q S}$, profile drag coefficient

Table 1

Description of the Figures

1. Photograph, static propeller test rig.
2. Diagram of static thrust and torque set-up.
3. Blade form curves.
4. Propeller blade sections at the 0.70 R.
- 5-8. Variation of static thrust and power with tip-speed ratio and blade angle.
- 9-18. Static propeller characteristics as functions of blade angle.
- 19-21. Comparisons of static thrust figures of merit.
22. Lift and drag coefficients computed from static propeller characteristics.
- 23-24. Envelope efficiencies computed by Driggs' method.

DISCUSSION

In this series of static propeller tests, made for comparing the Clark Y airfoil propeller section with the NACA 16-series section, the independent variables used were blade angle and propeller rotational speed. Blade angle was fixed for each test, hence changes in propeller characteristics during a run must be attributable only to changing propeller rotational speed. At least three factors which affect the behavior of the propeller blade airfoil sections are functions of the rotational speed. Of first importance is the increase with tip-speed ratio of the Mach number at which the blade sections work, and the changes in blade section airfoil characteristics with Mach number. A secondary effect of increase in rotational speed is an increase in the Reynolds number at which the blade sections work. A third factor, of unknown influence, is the tendency of the propeller blade to discard by centrifugal force the retarded air composing the boundary layer. Both of the latter two factors have a beneficial influence on the performance of the blade sections. Even at a tip-speed much below that for normal operation most of the propeller sections work at values of the Reynolds number greater than the critical; hence, as the Reynolds number is increased blade section profile drag coefficient is reduced and maximum lift coefficient is increased. The effect of centrifugal force on the air in the boundary layer may act to remove it, which would have the effect of delaying the normal stall.

Apparently the only adverse effect accompanying high propeller tip speed is due to the behavior of airfoils in compressible flow as the air speed approaches the velocity of sound. Wind-tunnel tests, reference 5, have shown that both the lift and drag coefficients of an airfoil increase with increasing Mach number until a critical value is reached. This value is believed to be reached when the local air velocity at some point on the airfoil is equal to the velocity of sound. As the Mach number is increased beyond the critical value the lift coefficient decreases while the drag coefficient increases more rapidly than it does at subcritical values of the Mach number. Only the net influence of the several factors is measured by static propeller tests. Therefore, the adverse effect of air compressibility on blade section behavior at high tip speed, being partially offset by beneficial factors, is not as fully discernible from static propeller tests as from wind-tunnel tests on airfoils.

While the tests were being made it was noticed during each run that the character of the noise emitted by the engine and propeller began to change from a roar to a penetrating note at about 1800 rpm. The propeller diameter was ten feet. This may indicate that the first shock waves are set up at the propeller tips at a tip speed ratio of about $M = 0.82$. The region of the propeller blade tip producing a shock wave spreads inwardly as the tip speed ratio increases. Since the highest value of the tip-speed ratio obtained in these tests was $M = 1.05$, only those sections at radii greater than $0.78 R$ were working at a value of Mach number greater than $M = 0.82$. The effect of compressibility indicated in the figures was produced in most cases by a relatively small outer portion of the propeller blades.

The basic pitch distribution for the propeller blades subject to these tests was 30° at the three-quarters radius. This pitch distribution will give highest propeller efficiencies within a range of advance ratio between $J = 1.3$ and $J = 2.0$. This high basic pitch distribution does not lend itself well to static propeller tests because of the great difference in angles of attack of the inboard sections from those of the tip sections. A high basic pitch distribution results in a tendency for a propeller in static tests to yield less thrust for a given power than a similar propeller with less blade twist. It is this fact which discredits the propeller polars and efficiency curves computed by the single-point method from the results of static tests, and confines their usefulness to qualitative comparisons.

The variation of static thrust coefficients with tip-speed ratio shown in figures 5 and 6 verifies the results of wind-tunnel tests on airfoils. The increasing static thrust coefficient with increasing tip-speed ratio indicates that, when blade sections near the tip are working at positive lift, the lift coefficients increase with increasing Mach number up to a certain point. The lower rate of increase of the static thrust coefficient as tip-speed ratios approach unity indicate a decrease of the lift coefficients of sections near the blade tip as the Mach number at which they operate approaches unity. The rapid rise of the static thrust coefficients with increasing tip-speed ratio produced at the high blade angles even at low values of the tip-speed ratio may be attributable to Reynolds number effect and to the beneficial action of centrifugal force in throwing off dead air from the stalled region of the propeller.

The variation of static power coefficient with tip-speed ratio, shown in figures 7 and 8, also agrees with wind-tunnel tests on airfoils. The slight decrease of the static power

coefficients with increasing tip-speed ratio at low values of the tip-speed ratio may be due to decreasing drag coefficients of the blade section with increasing Reynolds number. For the blade settings which yield positive lift near the tip, the gradually increasing power coefficients at tip-speed ratios of about $M = 0.7$ or $M = 0.8$ again indicate the increase of lift and drag coefficients of airfoils working at Mach numbers below the critical. The sharper rise of the power coefficients, for all blade settings, as the tip-speed ratio approaches unity, is comparable to the rapid increase of airfoil drag coefficients as the Mach number approaches unity:

Figures 9 to 18, inclusive, are cross plots of figures 5 through 8 at tip-speed ratios of $M = 0.5, 0.7, 0.9, 1.0,$ and 1.1 . The static thrust and power coefficients and static thrust figure of merit are shown as functions of blade angle at the three-quarters radius. The fact that the static thrust figures of merit for the 16-series sections reach maxima at slightly higher blade angles than the Clark Y sections may be accounted for by the higher angle of zero lift for the 16-series sections.

The relative merits of the two propeller sections may be shown best by comparison of properties independent of blade angle. Figures 19 through 21 present comparisons of the static thrust figures of merit of the Clark Y and 16-series sections plotted against power coefficient at values of the tip-speed ratio of $M = 0.5, 0.7, 0.9, 1.0,$ and 1.1 . These charts show that in general the 16-series sections are superior to the Clark Y sections over a limited range of operation. Inasmuch as the 16-series sections were specifically designed to operate efficiently at high speed the extent of their superiority shown by these static tests is disappointingly small. For both sections the values of the figure of merit reach a maximum at a tip-speed ratio between $M = 0.7$ and $M = 0.9$; hence, a propeller might be expected to operate most efficiently at a tip speed ratio of $M = 0.9$ or slightly less. Figure 19 shows that there is almost no choice between the sections at $M = 0.5$ and $M = 0.7$; the 16-series section appears better through a small range at low values of the power coefficient, and the Clark Y slightly superior for all higher values of the power coefficient.

The comparison of static thrust figures of merit in figure 20 is more favorable to the 16-series section. At $M = 0.9$ the values of the static thrust figure of merit for the 16-series section exceed those for the Clark Y section by an average of about four percent over a comparatively large range of values

of power coefficient. At $M = 1.0$ the superiority of the 16-series section averaged only about two percent, but in this case also the superiority held over a reasonably wide range of power coefficient values. Even at these tip-speed ratios, however, the superiority of the Clark Y section at high power coefficients, that is, under high loading, is unquestionable. Propeller efficiency is equal to the product of thrust figure of merit multiplied by advance ratio ($\eta = C_T/C_P \times J$). The value of the thrust figure of merit necessarily decreases as the advance ratio increases. If the relative values of the thrust figures of merit of the two sections do not change with advance ratio, about three percent greater efficiency may be expected of a propeller embodying the 16-series sections than from one made with Clark Y sections, when the value of tip-speed ratio is close to $M = 0.9$ or $M = 1.0$. In static tests the axial velocity through the propeller is relatively small. When a propeller is in actual operation advancing at a normal high speed, the blade section resultant velocity of rotation and advance is considerably higher than the velocity due to rotation alone and consequently the region of the propeller tip suffering a compressional loss extends considerably farther inboard. The propeller losses at high tip-speed ratios indicated by static tests will most likely be exceeded in flight.

The static thrust figures of merit presented in figure 21 indicate little difference between the behavior of the two sections at a tip-speed ratio of $M = 1.1$. Since all of the values at $M = 1.1$ were obtained by extrapolation, the comparison at this tip speed ratio is not conclusive.

The lift and drag coefficients computed by the method given in reference 2 from static propeller characteristics are presented as polars in figure 22. These of necessity yield the same information as the static thrust figure of merit comparisons, though in a more easily interpretable form. This method of propeller blade section analysis regards the propeller as an airfoil acting at the seven-tenths radius station. For both sections the value of minimum drag coefficient does not change much between values of tip-speed ratio of $M = 0.5$ to $M = 0.9$. The drag coefficients increase rapidly with tip-speed ratio when these values exceed $M = 0.9$. Maximum lift coefficient decreases continuously for both sections as the tip-speed ratio increases. The distinct early stall of the 16-series section again indicates the superiority under heavy loading of the Clark Y sections which attain higher lift coefficients and stall more gradually. This leads directly to the conclusion that the Clark Y propeller is superior to the 16-series propeller during take-off. This is in

agreement with the results of wind-tunnel tests reported in reference 1. The information obtained in the wind-tunnel at low values of the tip-speed ratio with regard to propeller stall during take-off apparently holds for all higher values of the tip-speed ratio. These polars do not represent absolute values of the airfoil characteristics, but are chiefly for the purpose of comparing the Clark Y and 16-series propeller sections. The unusually large values of the drag coefficients shown by these polars may be due both to the high pitch distribution of the propellers and to large impedance to the propeller slipstream by the cowling and nacelle.

The propeller polars shown in figure 22 have been used in applying Driggs' method for computing propeller efficiencies. Since the polars show only relative values, the computed efficiency curves likewise can show only relative values. The absolute values indicated near maximum efficiency are about ten percent lower than those obtained in wind-tunnel tests on the same propellers with a well streamlined body, reference 1. Figures 23 and 24 are comparisons of the computed envelope efficiency curves of two propellers identical in all respects except blade section. The assumed power available is that which may be obtained from a Pratt and Whitney R-2800 engine with the propeller geared to operate at one-half engine speed. In these computations the actual propeller tip-speed ratio was used rather than rotational tip-speed ratio.

Figure 23 presents relative efficiencies at sea level. Due to the low maximum lift coefficients obtainable with the 16-series sections, the Clark Y propeller is superior at the very low values of advance ratio encountered at take-off. At high values of the advance ratio where the blade sections work at lower lift coefficients and where the effect of compressibility becomes noticeable the propeller having 16-series sections is slightly more efficient.

A comparison similar to that just made is shown in figure 24 for the conditions obtainable at an altitude of 19,500 feet. Since air temperature decreases with increasing altitude, the acoustic velocity also decreases and consequently tip-speed ratios increase. True tip speeds also increase with altitude due to the higher forward speeds obtainable. Computations show that the propellers of airplanes now in use at high altitude may be operating at tip-speed ratios of $M = 1.2$ or higher. The lower pair of curves in figure 24 shows a comparison of propellers having 16-series sections and Clark Y sections operating at true tip-speed ratios. The Clark Y propeller is

still superior at low values of the advance ratio due to the small values of maximum lift coefficient obtainable with the 16-series sections. At higher values of the advance ratio, however, where the blade sections operate at lower lift coefficients the 16-series sections show their superiority. For the example taken the propeller operates at a tip-speed ratio of $M = 1.0$ when the value of the advance ratio is $J = 1.5$. At this point, $M = 1.0$, where the data obtained in these tests are fairly reliable, the 16-series sections show up favorably, yielding a propeller efficiency about three percent higher than can be obtained with the Clark Y sections. At higher values of the advance ratio, where the tip-speed ratio was as high as 1.2, the computations depended upon extrapolation considerably beyond the range of the test data and are therefore not reliable for comparing the two sections. Use of this extrapolated data, however, gives a fair indication of the trend of the propeller efficiency at high values of tip-speed ratio and advance ratio. The two upper curves in figure 24 were obtained by computations identical with those by which the lower curves were obtained except that the propeller polars for a tip-speed ratio of $M = 0.5$ were used. These curves show what relative propeller efficiencies could be obtained if there were no loss due to compressibility. The differences between the curves for a tip-speed ratio of $M = 0.5$ and the curves for the true tip-speed ratios indicate roughly the compressibility loss.

REMARKS

1. Both propellers gave highest values of the static thrust figure of merit at a tip-speed ratio between $M = 0.7$ and $M = 0.9$; hence, in flight highest efficiency may be expected in the same range of tip-speed ratios.
2. Propeller efficiency at high speed computed from these static propeller data indicates that at tip-speed ratios close to $M = 0.9$ the propeller having 16-series sections yields about three percent higher peak efficiency than the propeller embodying Clark Y sections.
3. The propeller having 16-series blade sections was found to stall at lower values of the lift coefficient than did the Clark Y propeller at all values of the tip-speed ratio. This agrees with low-speed wind-tunnel tests which indicate the superiority of the Clark Y propeller for take-off and climb. On the basis of these static tests the superiority of the Clark Y propeller for take-off and climb holds for all values of tip-speed ratio.

4. It is to be understood that the conclusions reached from these tests with regard to the 16-series sections apply only to sections designed to operate most effectively at lift coefficients between $C_L = 0.40$ and $C_L = 0.50$.

5. It is probable that better take-off and climb operation could be obtained from a 16-series propeller designed to operate best at higher values of the lift coefficient than those for which the subject propeller was designed.

6. Redesign of the 16-series propeller with greater blade area and for higher tip-speeds might produce a propeller with much better take-off characteristics with little sacrifice of efficiency at high speed.

Langley Memorial Aeronautical Laboratory,
National Advisory Committee for Aeronautics,
Langley Field, Va., August 28, 1941.

REFERENCES

1. Gray, W. H.: Wind-Tunnel Tests of Two Hamilton Standard Propellers Embodying Clark Y and NACA 16-Series Blade Sections. NACA MR, Aug. 20, 1941.
2. Driggs, Ivan H.: Simplified Propeller Calculations. Jour. Aero. Sci., vol. 5, no. 9, July 1938, pp. 337 - 344.
3. Hartman, Edwin P., and Biermann, David: Static Thrust and Power Characteristics of Six Full-Scale Propellers. NACA Rep. No. 684, 1940.
4. Stack, John: Tests of Airfoils Designed to Delay the Compressibility Burble. NACA TN No. 976, Dec. 1944. (Reprint of ACR, June 1939.)
5. Stack, John, Lindsey, W. F., and Littell, Robert E.: The Compressibility Burble and the Effect of Compressibility on Pressures and Forces Acting on an Airfoil. NACA Rep. No. 646, 1938.



Figure 1.- Static propeller test rig.

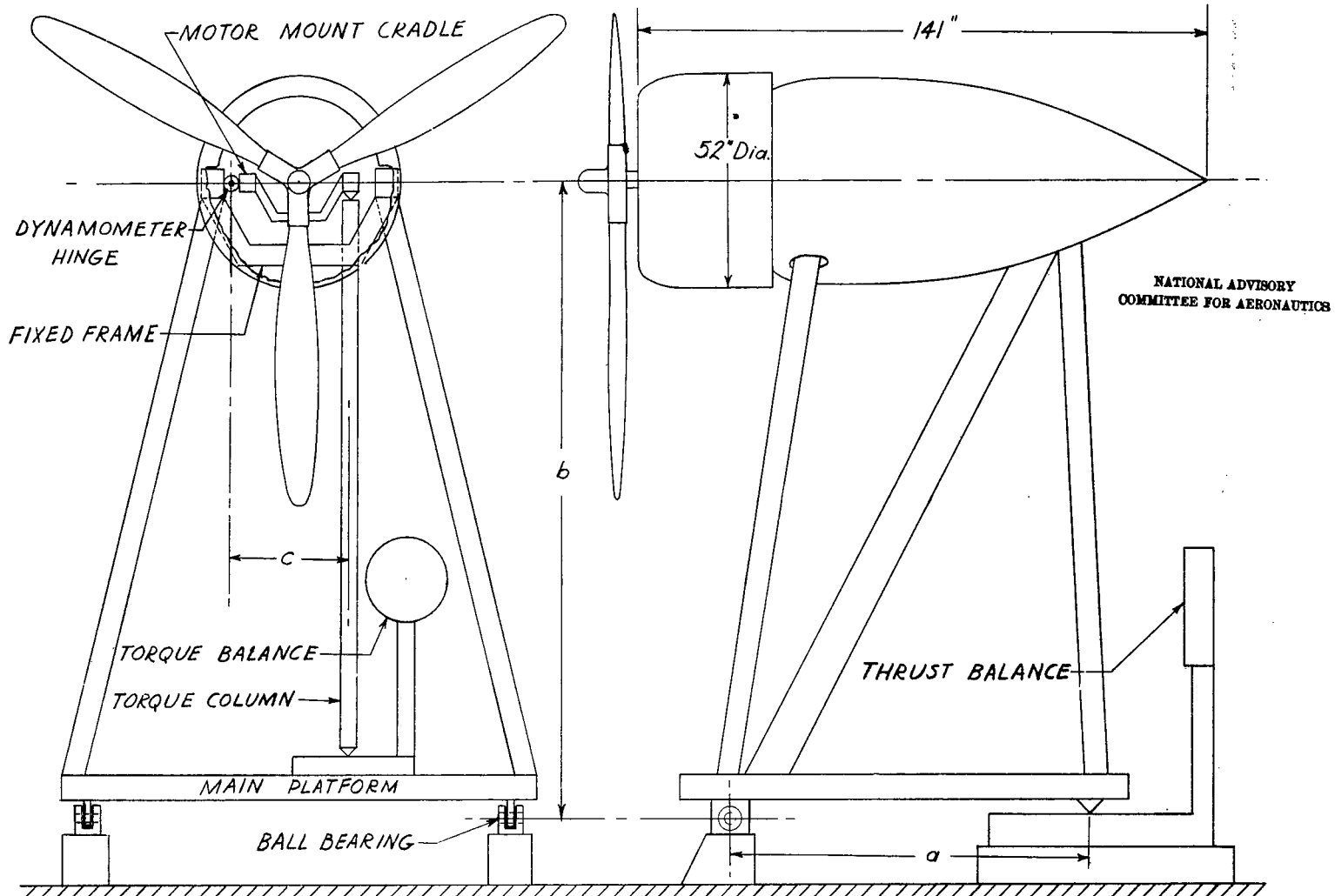
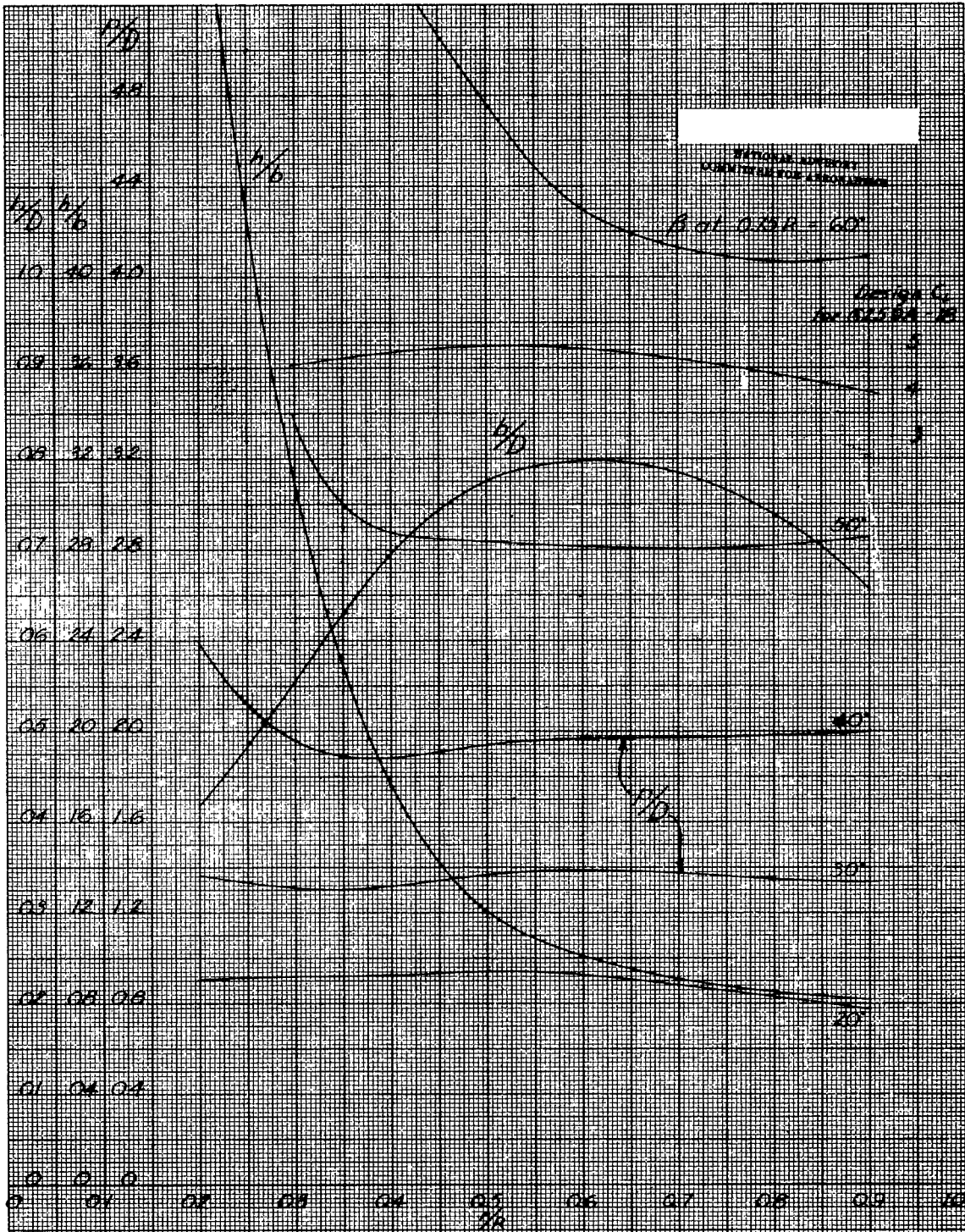


Figure 2.- Diagram of static thrust and torque set-up. -419-

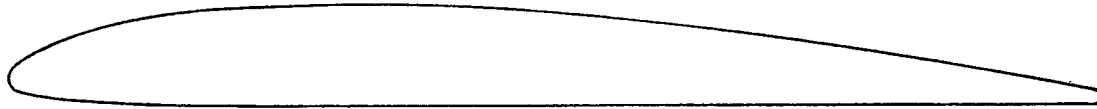


16-409

Figure 3-Blade form curves for Hamilton Standard propellers.
 6250A-18 & 6267A-18. D, diameter; R, radius to tip;
 r, section radius; c, section chord; h, section thickness;
 p, geometric pitch; β , blade angle.



No. 6259A-18, NACA 16-series



No. 6267A-18, Clark-Y

Figure 4 - Propeller blade sections at the 0.70 R.

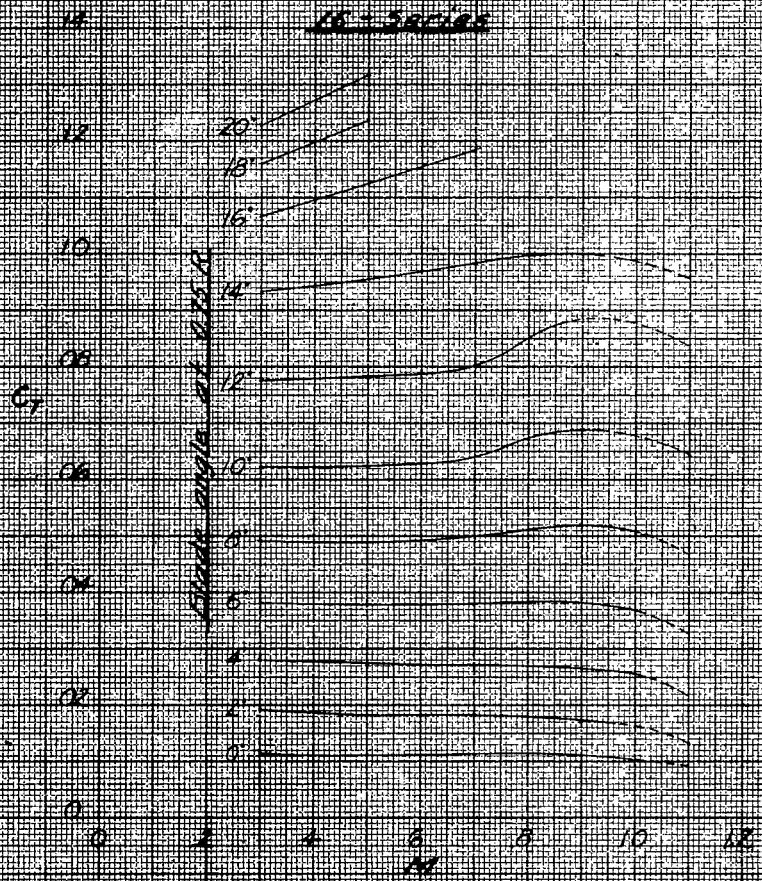


Figure 5 - Variation of static thrust coefficient with tip speed ratio and blade angle. Three bladed propeller No. 6253 A-18.

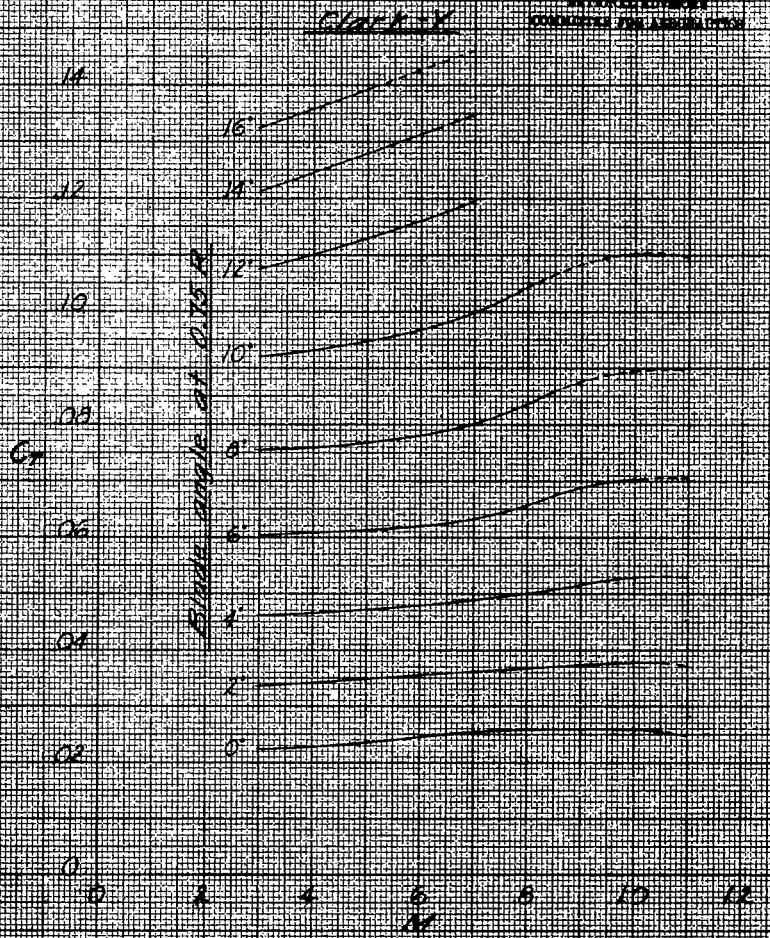


Figure 6 - Variation of static thrust coefficient with tip speed ratio and blade angle. Three bladed propeller No. 6267 A-18.

16-58113

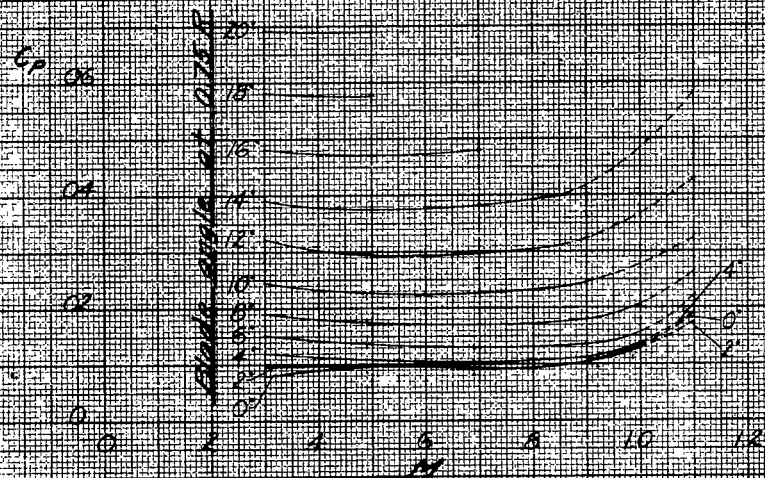


Figure 7 - Variation of static power coefficient with tip speed ratio and blade angle. Three bladed propeller No. 6253 A-18.

6166-1

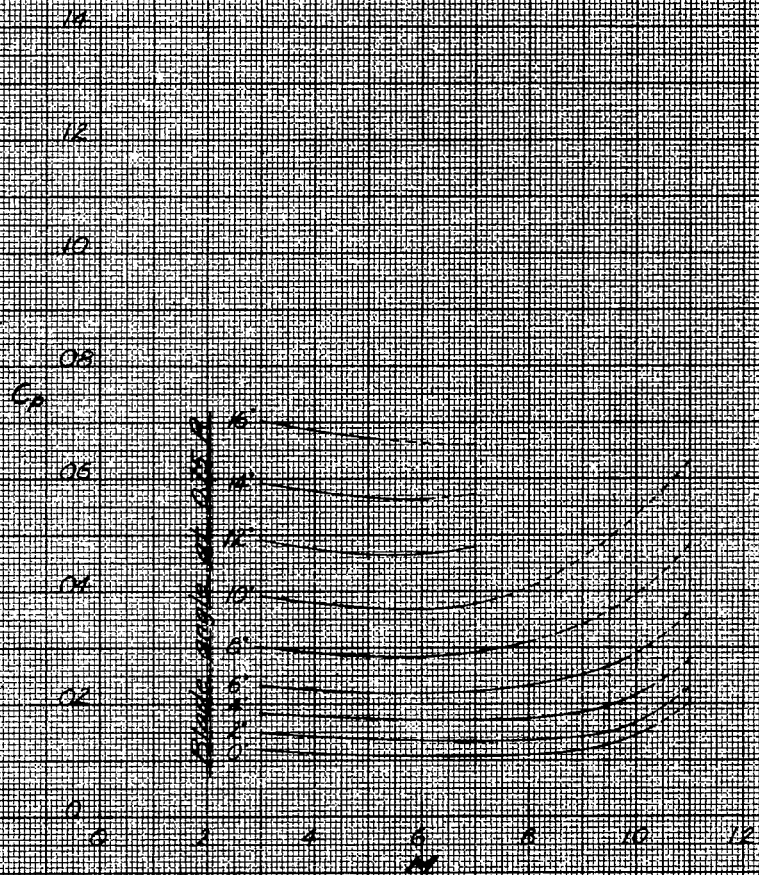


Figure 8 - Variation of static power coefficient with tip speed ratio and blade angle. Three bladed propeller No. 6267 A-18.

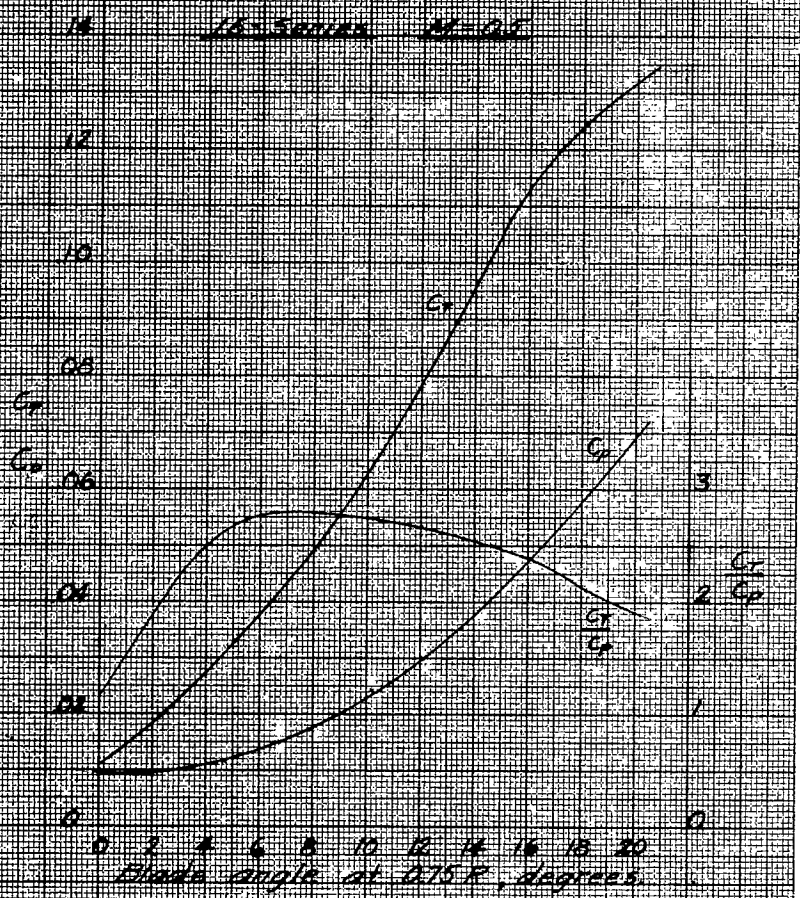


Figure 9 - Static propeller characteristics
 Three bladed propeller No. 6259A-18

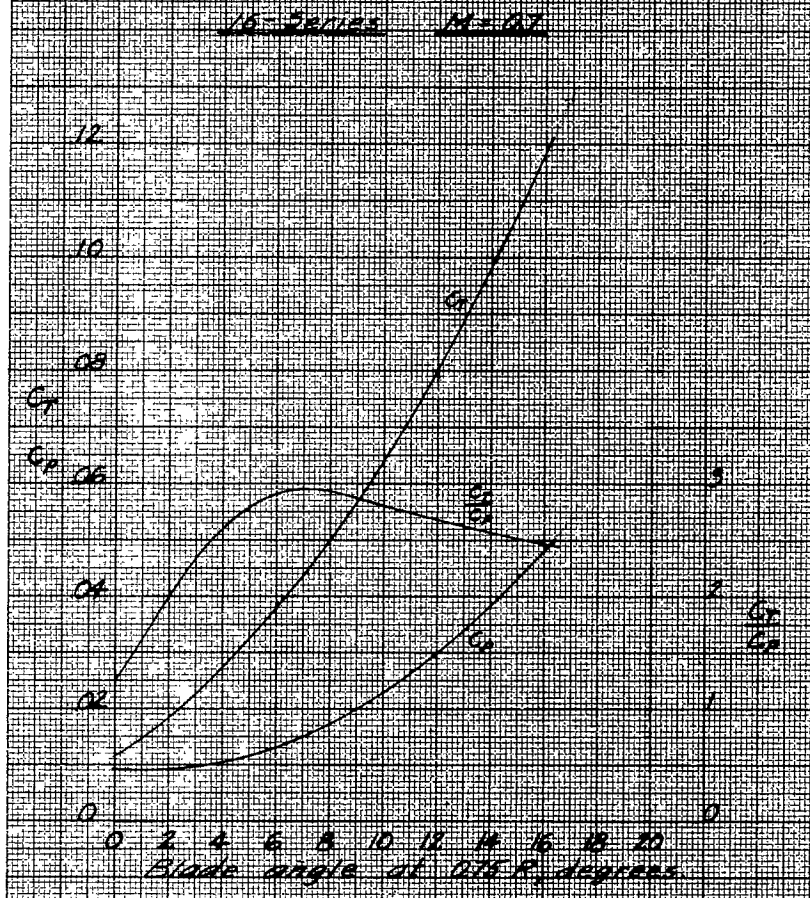


Figure 10 - Static propeller characteristics
 Three bladed propeller No. 6259A-18

✓

1A 16-Series $M=0.9$

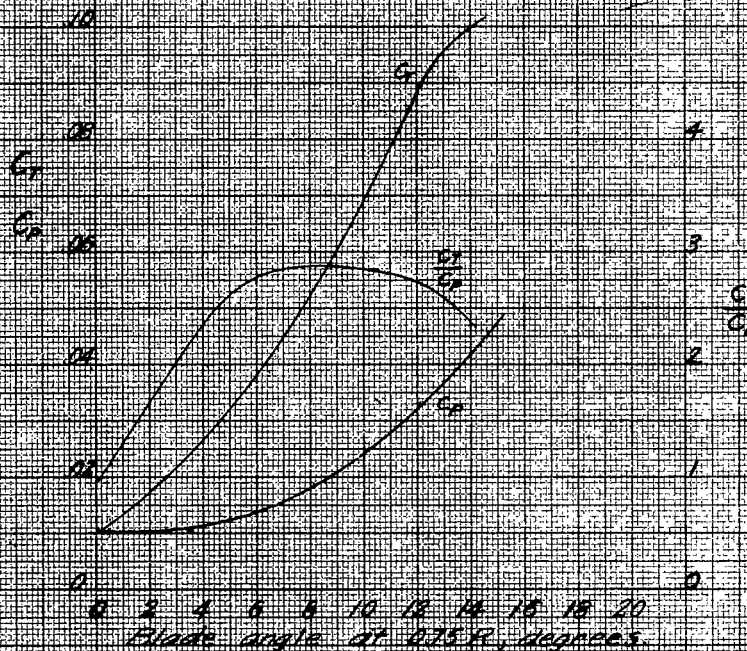


Figure 11. Static propeller characteristics.
Three-bladed propeller No. 6259A-19.

1A 16-Series $M=1.0$

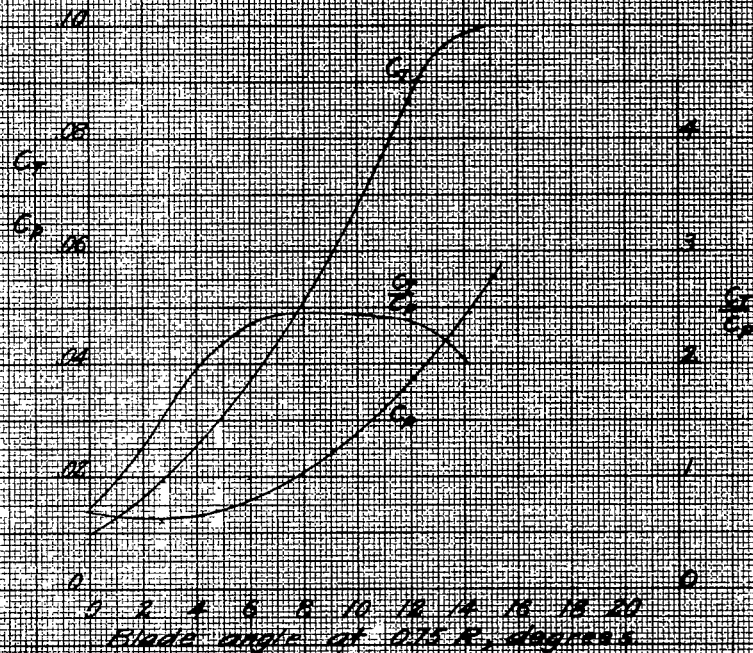


Figure 12. Static propeller characteristics.
Three-bladed propeller No. 6259A-19.

14 16 Series $M=14$
All values extrapolated

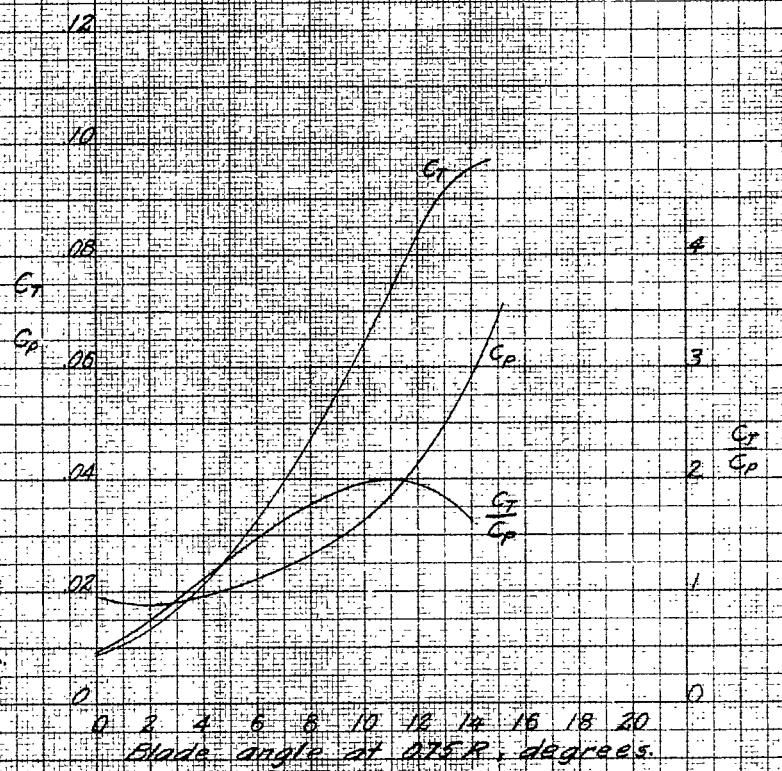


Figure 13 - Static propeller characteristics.
Three bladed propeller No. 6259A-18.

14 Clark-Y $M=0.5$

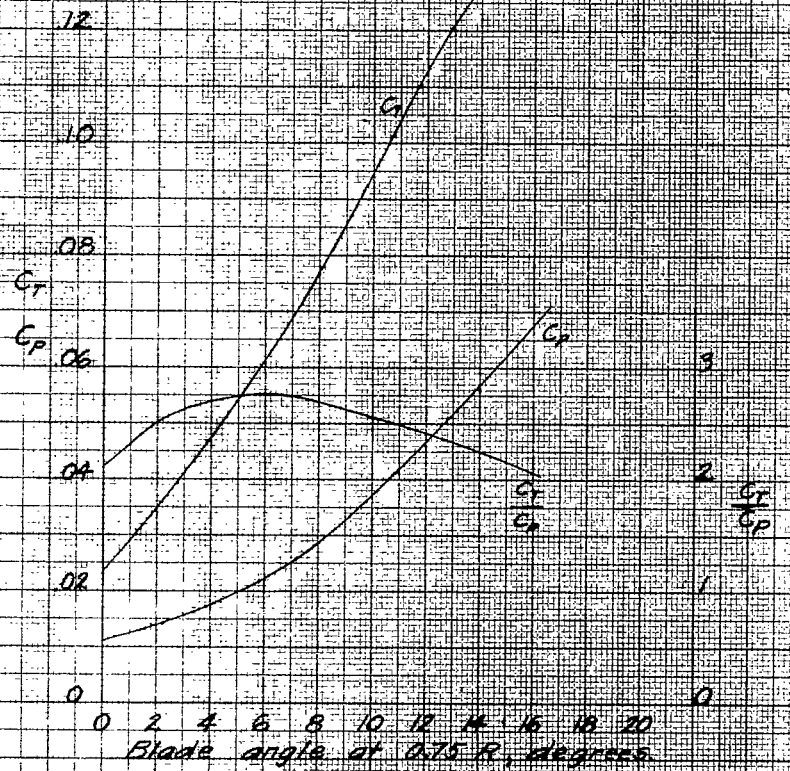
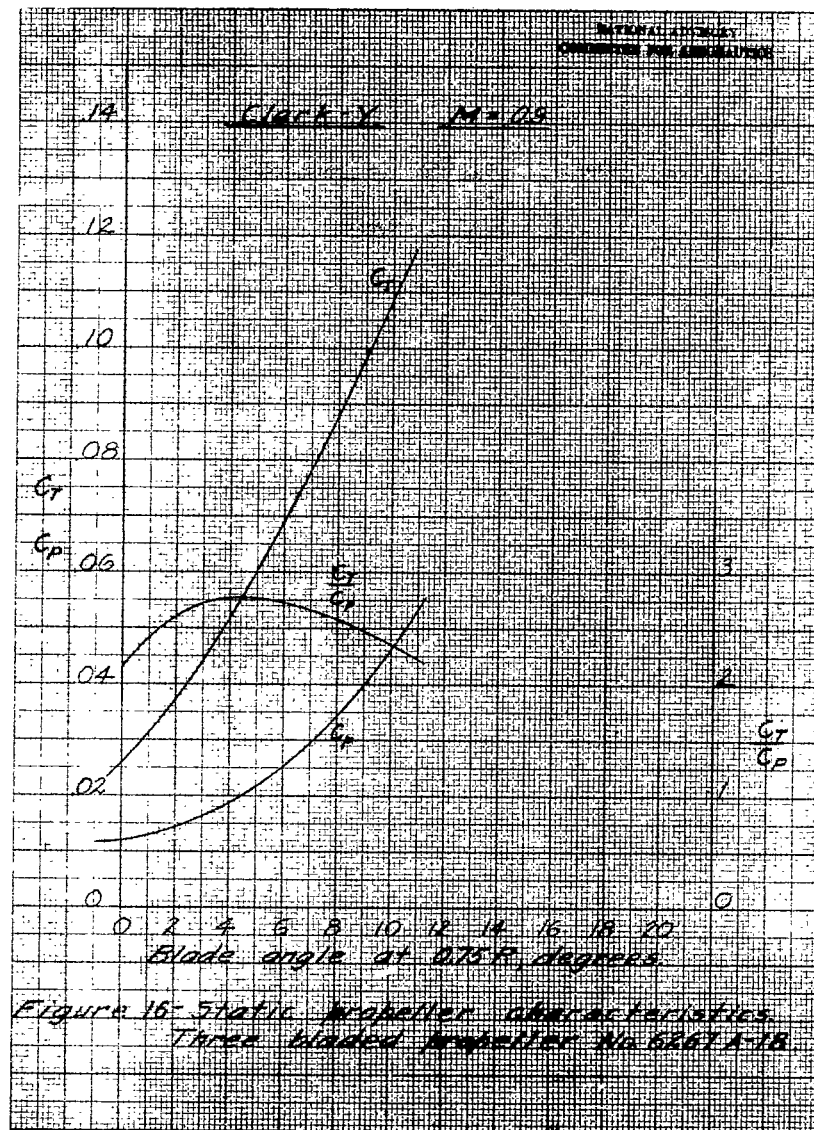
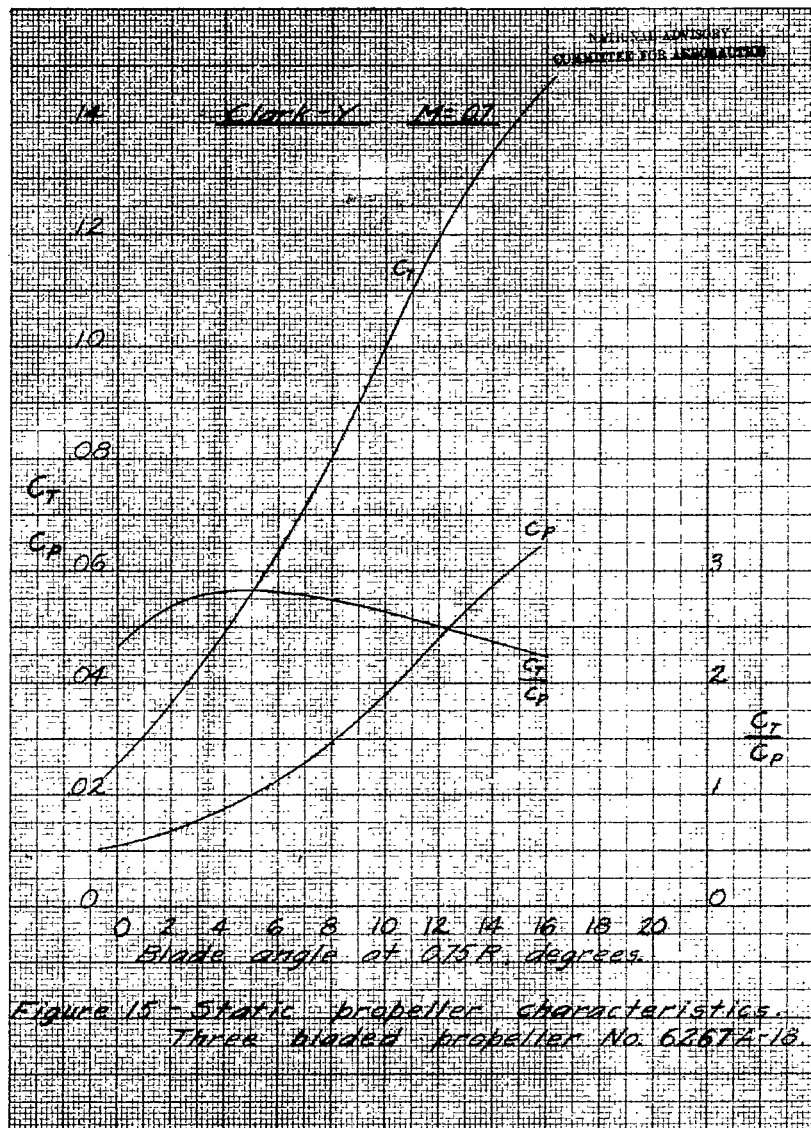


Figure 14 - Static propeller characteristics.
Three bladed propeller No. 6267A-18.



14 Clark-Y $M=10$

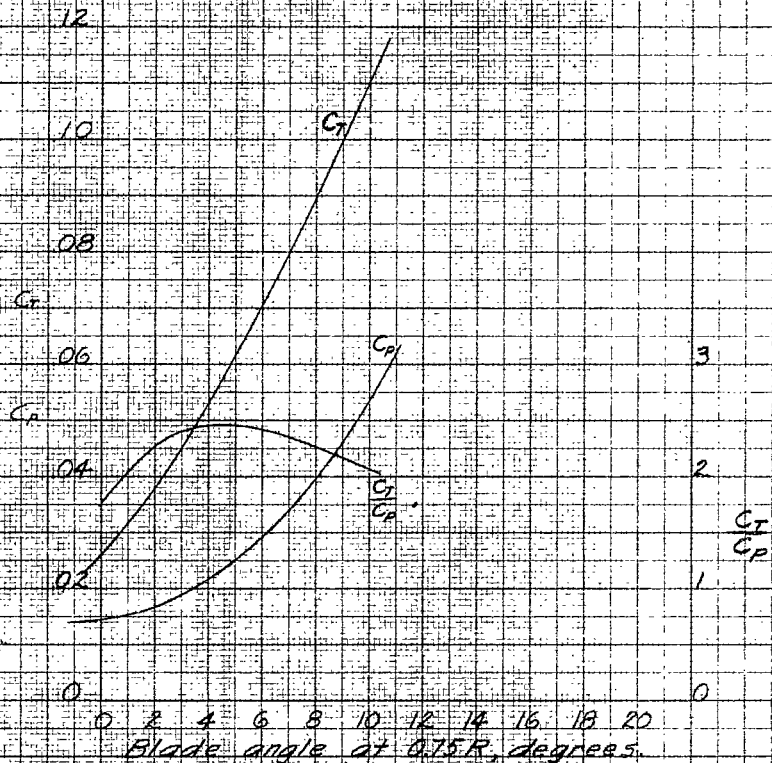


Figure 17 - Static propeller characteristics.
Three bladed propeller No. 6267A-18.

14 Clark-YC $M=11$

All values extrapolated

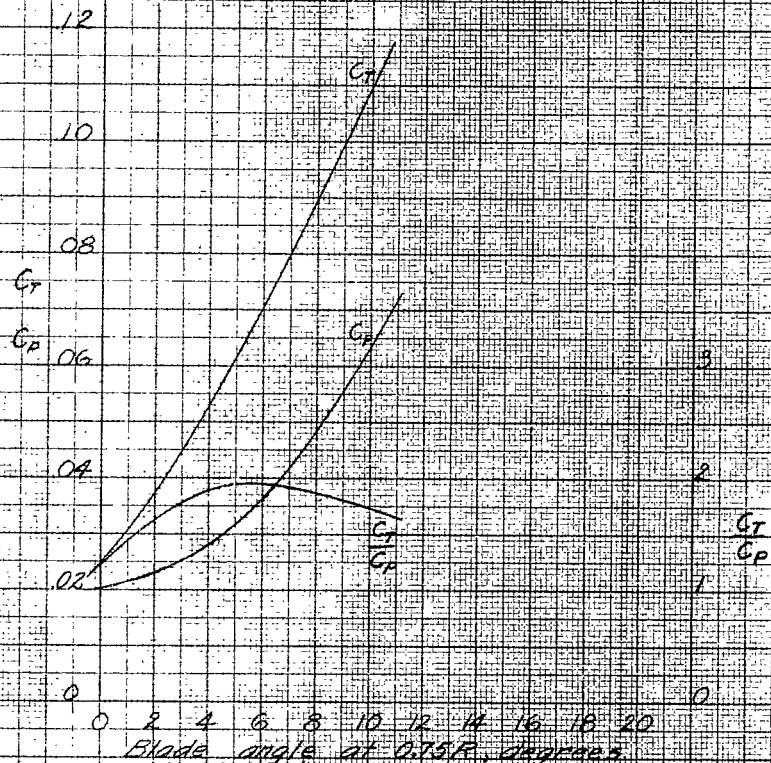
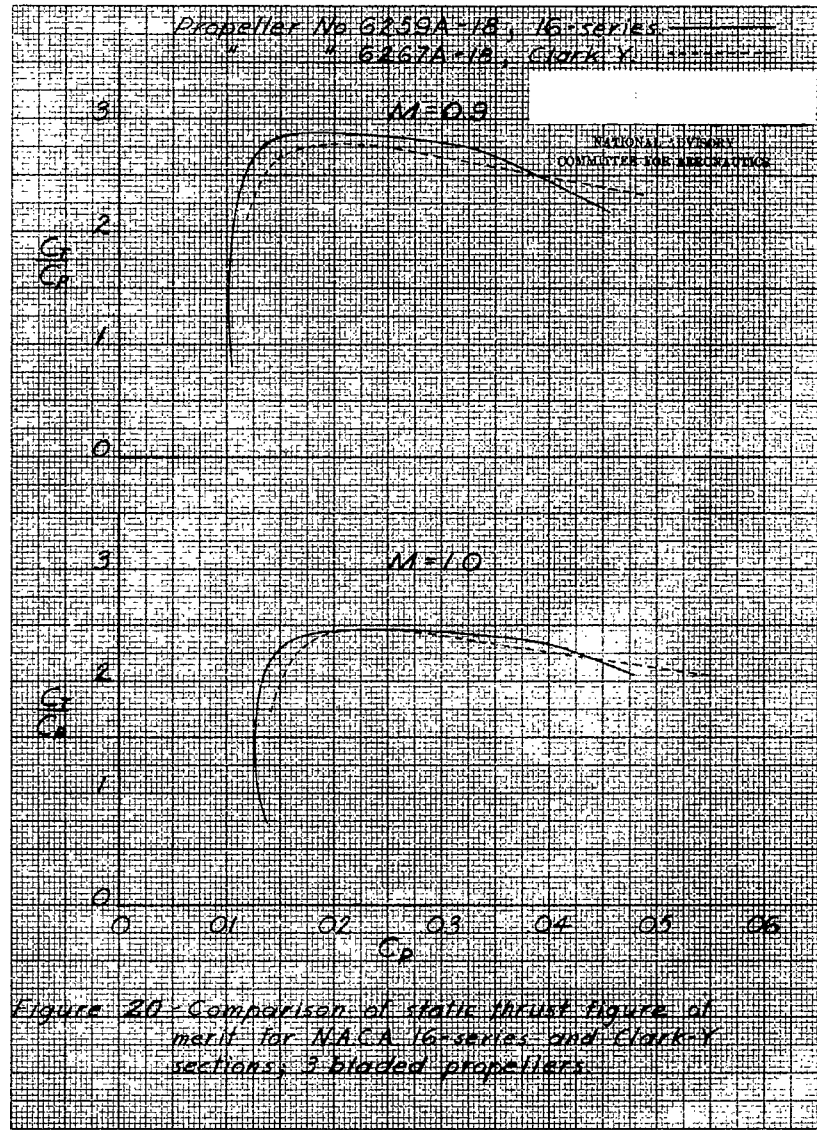
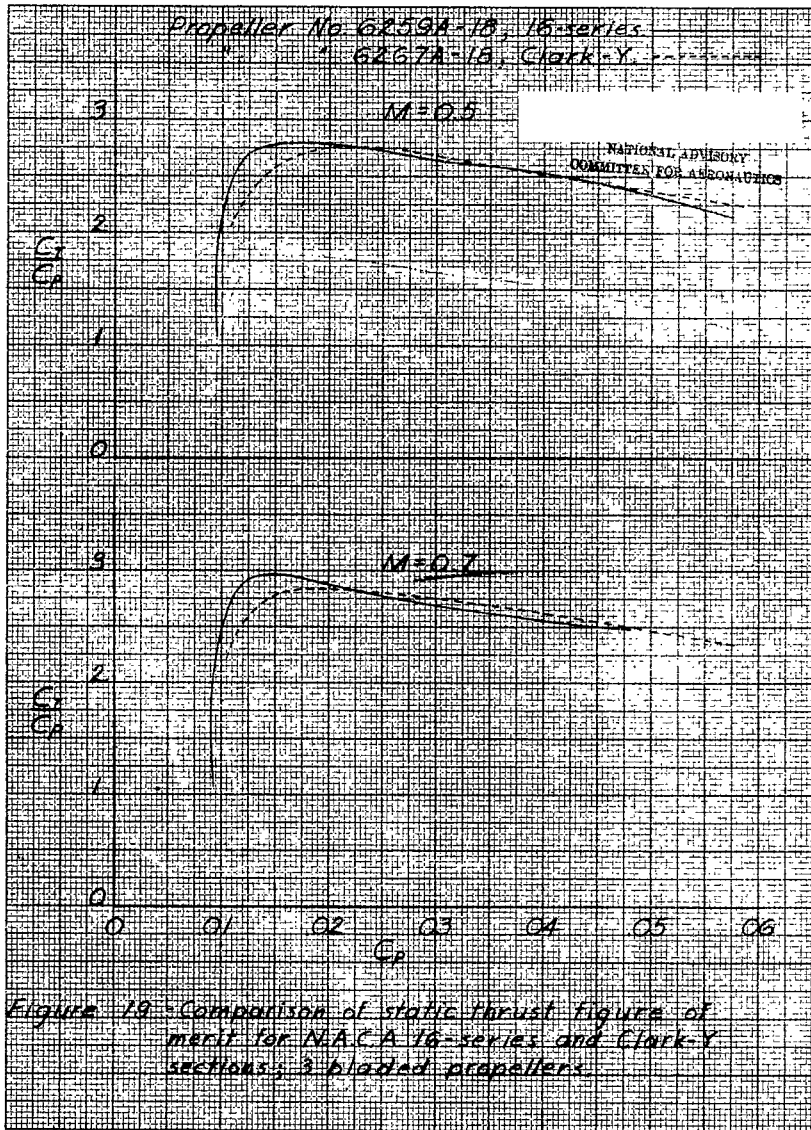


Figure 18 - Static propeller characteristics.
Three bladed propeller No. 6267A-18.



Propeller No. G259A-18, 16 series
" " G267A-18, Clark Y

M-11

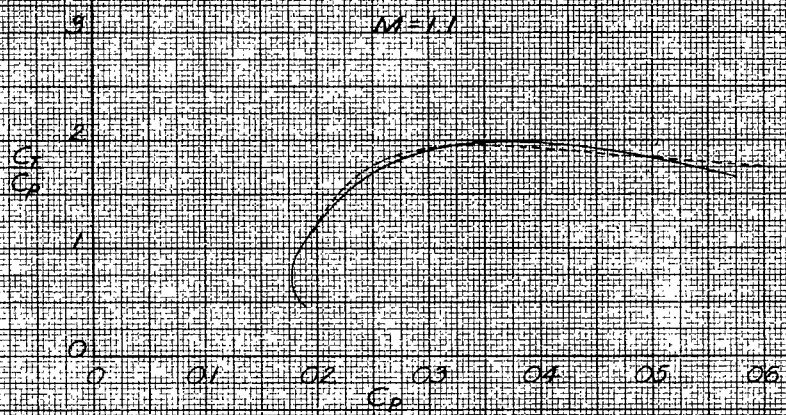
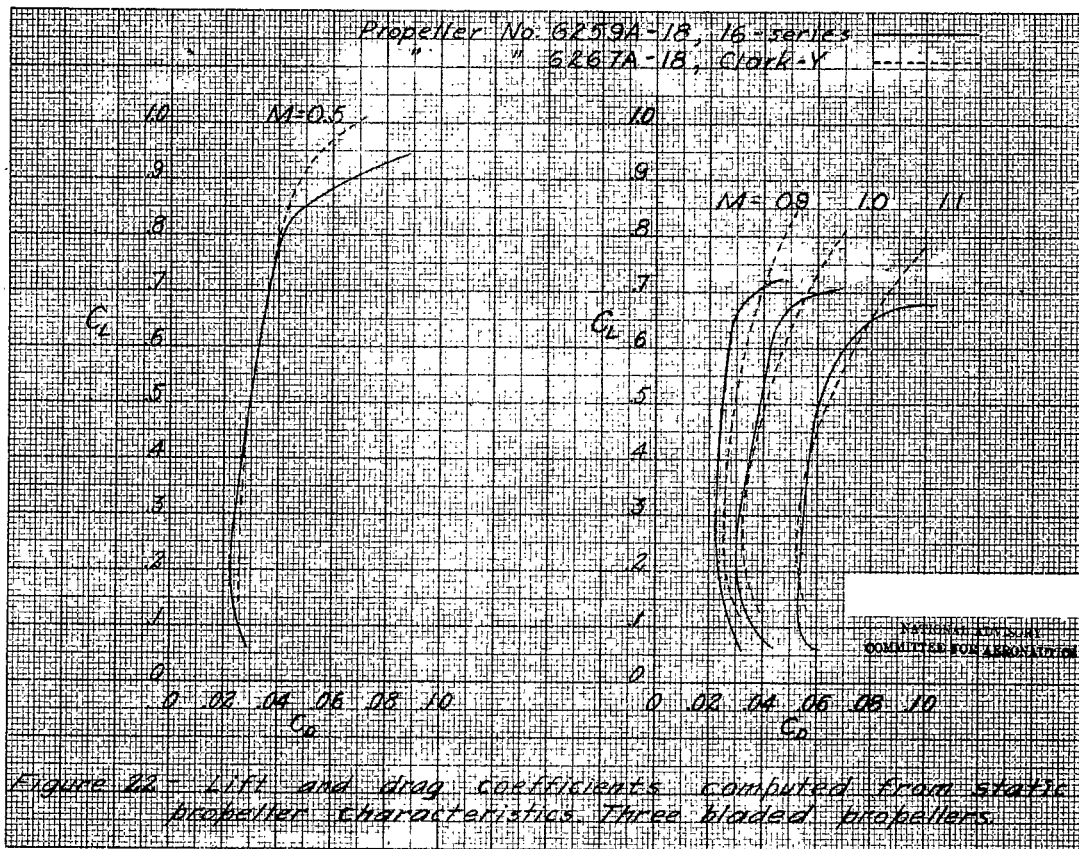


Figure 61 - Comparison of static thrust figure of merit for NACA 16-series and Clark Y sections; 3 bladed propellers



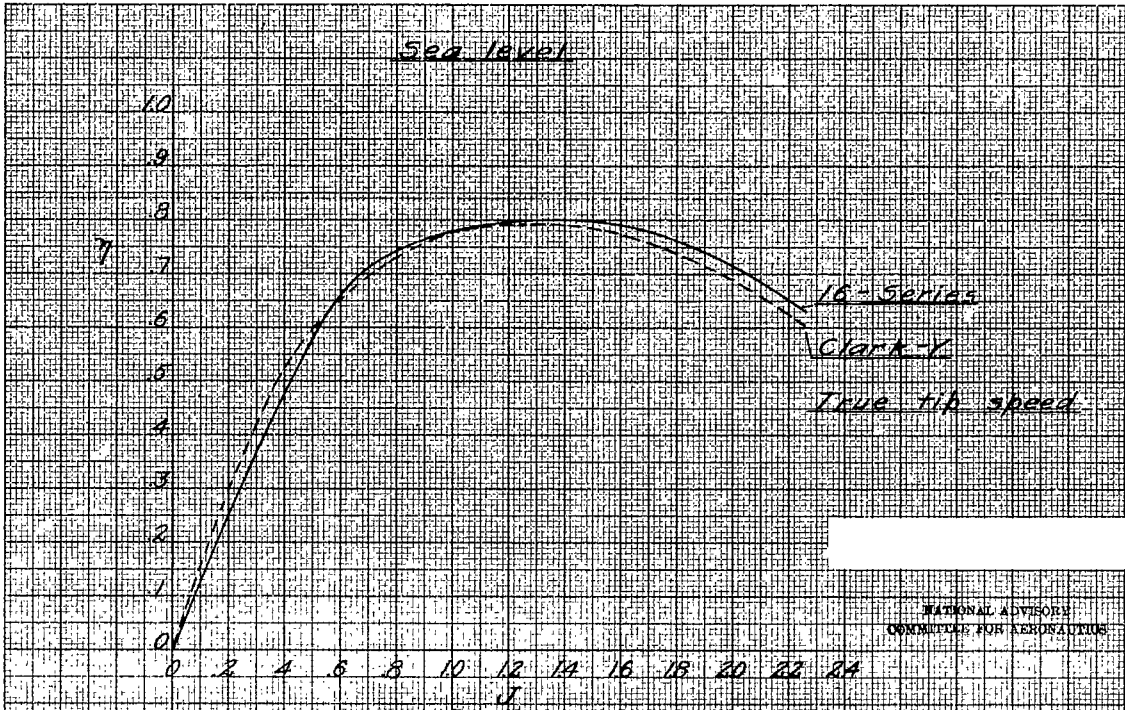


Figure 23-Envelope efficiencies computed by Prigg's method, 2000 hp, 1350 propeller rpm, 13.5 Ft diameter three bladed constant speed propeller.

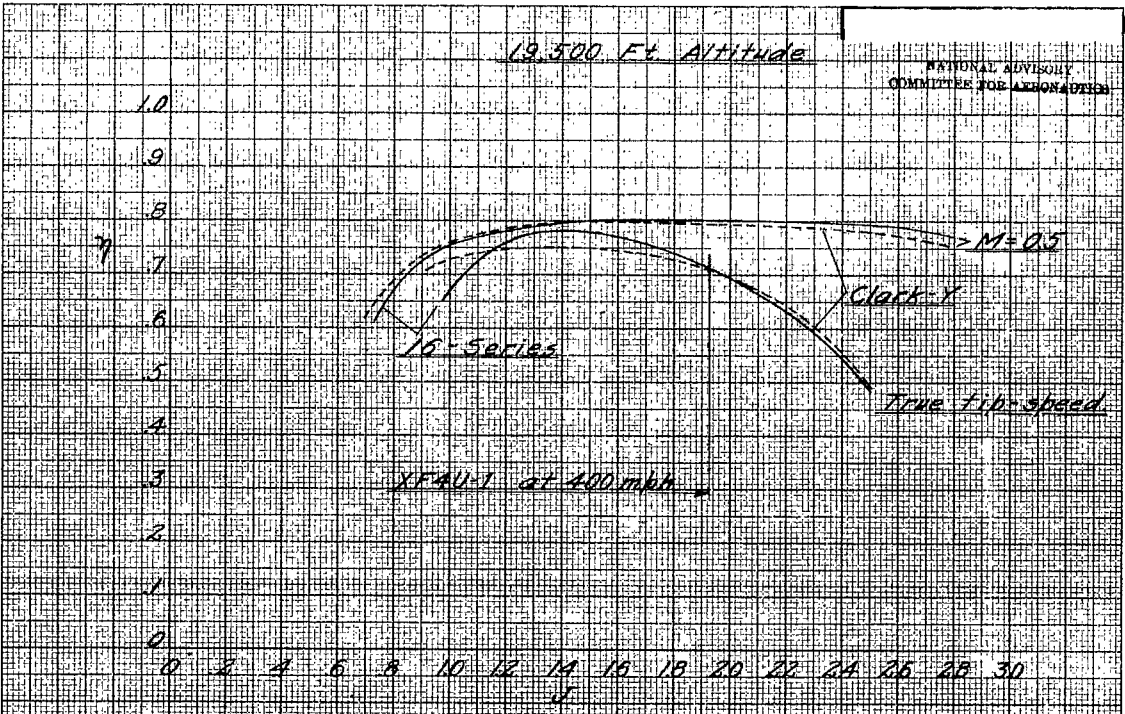


Figure 24-Envelope efficiencies computed by Prigg's method, 1800 hp, 1350 propeller rpm, 13.5 Ft diameter three bladed constant speed propeller.

LANGLEY RESEARCH CENTER



3 1176 01363 9936